

Phonons in the mixed crystal $\text{CdCl}_{2(1-x)}\text{Br}_{2x}$: n -mode behavior ($n \geq 10$)

R. W. G. Syme* and D. J. Lockwood

Division of Microstructural Sciences, National Research Council, Ottawa, Canada K1A 0R6

N. L. Rowell

Division of Physics, National Research Council, Ottawa, Canada K1A 0R6

K. S. Chao

Department of Physics, University of Canterbury, Christchurch, New Zealand

(Received 30 June 1986)

The Raman spectrum of the mixed layered compound $\text{CdCl}_{2(1-x)}\text{Br}_{2x}$ shows a complicated structure at frequencies between the corresponding A_{1g} and E_g phonon frequencies observed in isostructural CdCl_2 and CdBr_2 . This Raman structure has a marked concentration dependence. General features of the results have been successfully described in terms of a simple model that predicts a *ten-mode* behavior for the Raman-active phonons in the mixed crystal. Particular features in the spectrum suggest that preferred clusters of Cl^- or Br^- ions occur in the mixed-crystal lattice, probably as a result of a difference in lattice constants of the two components.

I. INTRODUCTION

Studies of phonons in mixed crystals of compounds possessing relatively simple structures have usually revealed a concentration dependence that is classified as one- or two-mode behavior.^{1,2} In one-mode behavior, the frequency of the phonon shifts with concentration from one limit to the other and only one peak is observed for that phonon in the vibrational spectrum of the mixed crystal. In two-mode behavior, two peaks are observed in the mixed-crystal spectrum for each active vibrational mode of the pure system and the intensities of the peaks vary with concentration so that they vanish at their respective concentration limits. More recently, three-mode behavior has been observed³⁻⁵ in mixed crystals of $\text{Hg}_2(\text{Cl}_x\text{Br}_{1-x})_2$, $\text{HfS}_{3-x}\text{Se}_x$, and $\text{GaS}_{1-x}\text{Se}_x$ where the results have been interpreted using the cell-type uniform displacements model.⁶ A basic condition for the success of this model is that the dispersion of the optical branches be small.

Even when further spectral structure is evident, some authors have preferred to describe the mixed-crystal situation as "one-mode" or "two-mode" behavior⁷ (or alternatively, "one-band" or "two-band" behavior⁸). However, where there is a clear resolution of extra spectral features, it would seem more appropriate to speak of " n -mode" or "multimode" behavior. In such a description n gives the number of clearly identifiable frequency components in the mixed-crystal spectrum associated with *each* active mode in a pure crystal. While the actual frequency of a given component may vary somewhat with crystal composition, the multimode description implies an ability to track each component (by intensity and possibly polarization) through some portion of the concentration range.

We report here the results of a Raman study of the mixed crystal $\text{CdCl}_{2(1-x)}\text{Br}_{2x}$. Cadmium chloride and cadmium bromide possess the same trigonal crystal struc-

ture, space group D_{3d}^5 , comprising layers of $X\text{-Cd-X}$ sandwich units stacked along the c axis.⁹ The optical phonons in these crystals exhibit weak dispersion,¹⁰ particularly along the c -axis direction, because of the nature of the bonding forces in the crystal. There is strong ionic bonding between the metal and halogen ions within a sandwich unit, and weak van der Waals bonding between halogens on different sandwich units. A factor group analysis¹¹ shows that the Raman spectrum of CdCl_2 or CdBr_2 comprises two modes; one of A_{1g} symmetry and one of E_g symmetry, with Raman tensors:

$$\begin{array}{c} A_{1g} \\ \left[\begin{array}{c} a \\ a \\ b \end{array} \right] \end{array} \quad \begin{array}{c} E_g \\ \left[\begin{array}{cc} c & d \\ -c & d \\ d & \cdot \end{array} \right] \end{array} \quad \begin{array}{c} E_g \\ \left[\begin{array}{ccc} \cdot & -c & -d \\ -c & \cdot & \\ -d & & \cdot \end{array} \right] \end{array}$$

Both of these modes have been measured previously.^{11,12} Thus $\text{CdCl}_{2(1-x)}\text{Br}_{2x}$ provides an example of a mixed crystal with a simple structure, and hence few optical modes, for which either one-mode or two-mode behavior might have been expected. The experimental results reported here, however, indicate an extremely complicated situation of multimode behavior, with the number of modes greater than or equal to 10. In contrast, we note that studies of mixed- CdCl_2 -type crystals of the form $M_{1-x}M'_xX_2$ (e.g., $\text{Cd}_{1-x}\text{Co}_x\text{Br}_2$, $\text{Fe}_{1-x}\text{Mn}_x\text{Cl}_2$, $\text{Fe}_{1-x}\text{Co}_x\text{Cl}_2$) revealed a simple one-mode behavior for the Raman-active phonons.¹³⁻¹⁵

The organization of the paper is as follows. In the next section we describe the experiments, and the results obtained are presented in Sec. III. A theory based on a molecular model is developed in Sec. IV, and then compared with experiment in Sec. V. Conclusions are drawn in the final section.

II. EXPERIMENT

The lattice constants for CdCl_2 and CdBr_2 in the larger hexagonal unit cell are $a'_0 = 3.85$ Å, $c'_0 = 17.46$ Å, and $a_0 = 3.95$ Å, $c_0 = 18.67$ Å, respectively.⁹ The constants for the two crystals are sufficiently similar that large, single crystals of $\text{CdCl}_{2(1-x)}\text{Br}_{2x}$ could be grown for any x value. The crystals were grown from the melt using the Bridgman-Stockbarger technique. Raman samples were prepared by cleaving sections from the crystal boules, and each sample was later analyzed for bromine and chlorine content by potentiometric titration with AgNO_3 . The nine samples used in our study proved to have x values of 0.01, 0.09, 0.29, 0.44, 0.52, 0.66, 0.73, 0.90, and 0.98, respectively.

Each sample was mounted in a Thor S500 cryostat where the sample is cooled by conduction and helium-exchange gas. The surface temperature of the crystal was measured using a gold-iron—Chromel thermocouple. In the Raman experiments 50 mW of filtered argon-laser light at either 457.9 or 476.5 nm was directed along an arbitrary axis (X) in the crystal ab plane, while the scattered light was collected at 90° to this along the c (Z) axis, normal to the cleavage plane. The scattered light was analyzed with Polaroid film, dispersed with a Spex 14018 double spectrometer at a spectral resolution of 3 cm^{-1} and detected with a cooled RCA 31034A photomultiplier. Spectra were recorded under computer control.¹⁶ Laser heating of the sample was not a problem in these experiments because the samples are optically transparent in the visible region. A weak fluorescence observed at 10 K with 476.5-nm excitation was avoided by using the 457.9-nm line. Some early Raman experiments¹⁷ were performed

with other equipment¹⁸ using the 476.5-nm argon-laser line, with essentially similar results. However, no polarization measurements were possible in this early work because of severe depolarization of the scattered light.

III. RESULTS

Typical results obtained from one sample for the temperature dependence of the scattered light are shown in Fig. 1. The main effect of reducing the temperature is seen in the widths of the lines, so that by 80 K, the multip peaked structure of the scattering in the mixed crystals is more evident. The relative intensities of lines also change with temperature, especially at lower frequencies, because of the change in the thermal population factors.

In Fig. 2, we show results obtained from another sample for the polarization characteristics of the scattered light. According to group theory (see Sec. I) scattering of E_g symmetry is allowed in all four measured polarizations with intensity $I_{YY} = I_{YX} \neq I_{ZX} = I_{ZY}$, while that of A_{1g} symmetry should appear only in (YY) polarization. This group-theoretical prediction strictly applies only to the pure crystals. In the mixed crystals, disorder obviates strict application of group-theoretical methods. Nevertheless, the polarization results obtained for the pure and mixed crystals are very similar. Lines at frequencies greater than approximately 135 cm^{-1} show strongly in (YY) polarization compared with (YX) polarization, while lines to lower frequency have a similar intensity in both polarizations. In the pure crystals¹² this information identifies the higher and lower frequency lines as having A_{1g} and E_g symmetry, respectively. Furthermore, the lower-frequency scattering appears with similar intensity

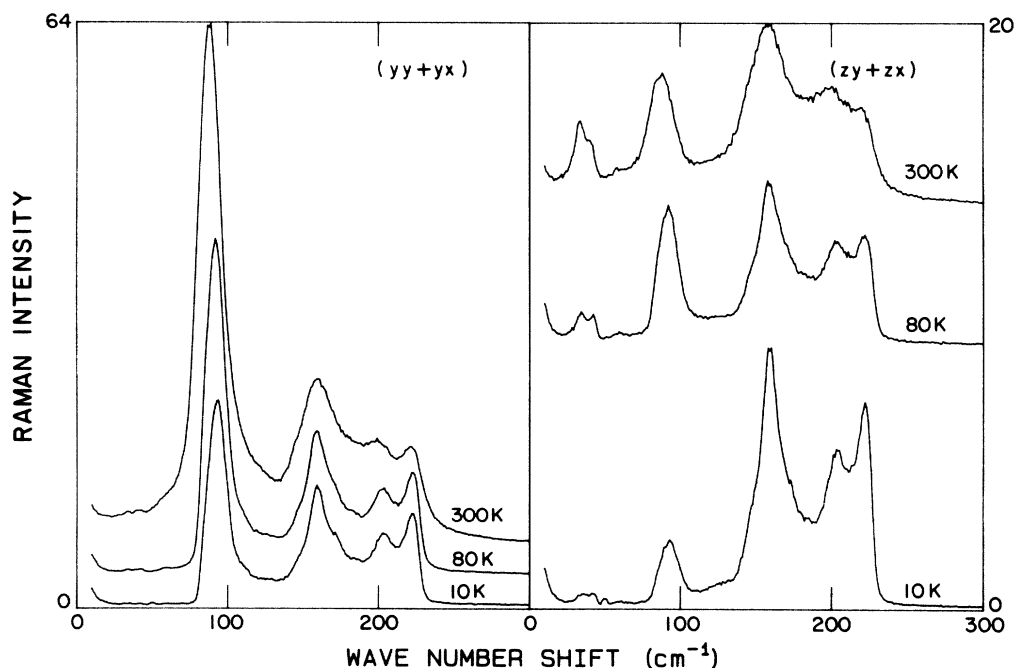


FIG. 1. Temperature dependence of the Raman spectrum of $\text{CdCl}_{0.96}\text{Br}_{1.04}$. The 300- and 80-K spectra were excited with 476.5-nm laser radiation and the 10-K spectrum with 457.9-nm radiation. The weak peak at 50 cm^{-1} in the 10-K spectrum is a laser plasma line.

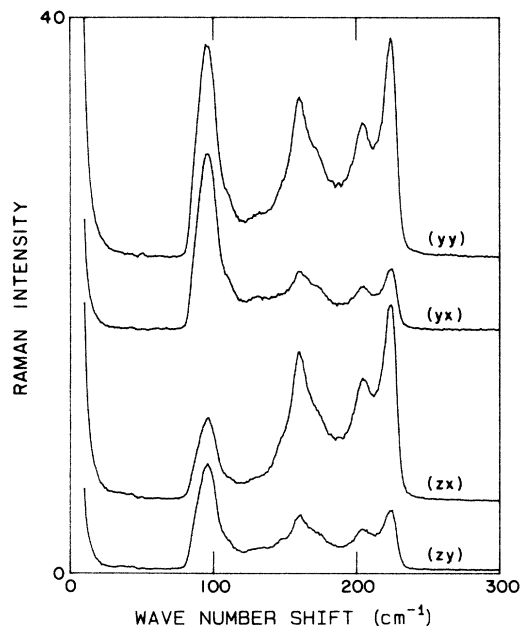


FIG. 2. Polarization dependence of the Raman spectrum of $\text{CdCl}_{1.12}\text{Br}_{0.88}$ recorded at 10 K with 457.9-nm laser excitation.

in (ZX) and (ZY) polarizations in the mixed crystals, as expected for the pure crystal, and is consistently weaker than that in (YY) or (YX) polarization. This indicates that a pseudo point symmetry of C_3 (or higher) governs the light scattering in the mixed crystals. The scattering is, therefore, still classified as having A and E symmetry. As Fig. 2 shows, the expected polarization selection rules are not well obeyed in practice because of depolarization of the light by the uniaxial crystal. For example, the A scattering-intensity ratio I_{YY}/I_{YX} , which should be infinity, was usually between 2 and 3 in these experiments, with no significant improvement for the nearly pure cases ($x=0.01$ and 0.98).

Because it was found experimentally that the pure-crystal polarization selection rules are still obeyed in the mixed crystals, it proved possible to separate clearly the A and E parts of the spectrum by scaling and subtraction of spectra. The (YX) spectrum was subtracted from the (YY) spectrum (with minor scaling being required in some cases) to reveal the pure A spectrum. This spectrum was scaled and subtracted in turn from the (YX) spectrum to produce the E spectrum. The result of this process, carried out for all concentrations, is shown in Figs. 3 and 4. Various spikes and other noisy features in these spectra result from the subtraction process. In Fig. 5 we show the concentration dependence of the (ZX,ZY) polarized Raman spectrum. This spectrum should contain E symmetry phonons only, but it also shows a significant A symmetry contribution because of the depolarization effects mentioned earlier. In Figs. 3–5 the $x=0.66$ spectrum is weaker than might be expected when compared with adjacent concentrations. This is a result of a poor optical quality sample which also produced the high depolarization evident in Fig. 5 for $x=0.66$.

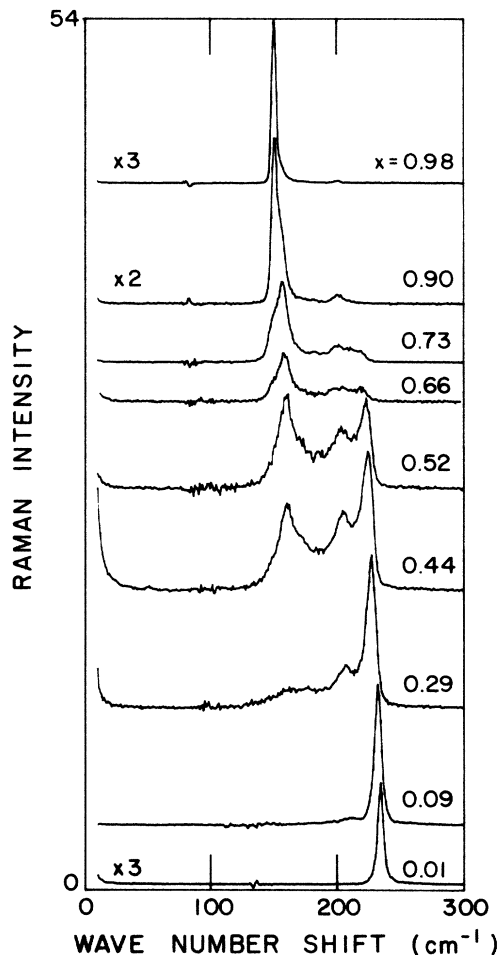


FIG. 3. Concentration dependence of the A -symmetry Raman spectrum of $\text{CdCl}_{2(1-x)}\text{Br}_{2x}$ recorded at 10 K with 457.9-nm laser excitation.

IV. THEORY

Theoretical studies of phonons in mixed crystals usually provide a description of the number of modes expected and predict the concentration dependences of their frequencies. Such studies have been fairly successful in reproducing the observed behavior in simple systems, but are difficult to apply in a more complicated case such as $\text{CsCo}_{1-x}\text{Mg}_x\text{Cl}_3$.¹⁹ In these cases, where there are many normal modes, it is difficult enough to predict the number of modes expected, let alone their concentration dependences. Fortunately, $\text{CdCl}_{2(1-x)}\text{Br}_{2x}$ is a simple case, with the pure crystals possessing only four optical modes of vibration,¹² two Raman-active (A_{1g}, E_g) and two infrared-active (A_{2u}, E_u). Application of the cell isodisplacement models¹⁻³ appropriate for this system results in three types of cell (Cl-Cd-Cl, Cl-Cd-Br, and Br-Cd-Br) which can at most produce a three-mode behavior for each optical mode. As Figs. 3 and 4 show, however, the experimental results are more complicated than this and a more elaborate model is required. In this section we develop what we shall call an averaged-nearest-neighbor (ANN) model.

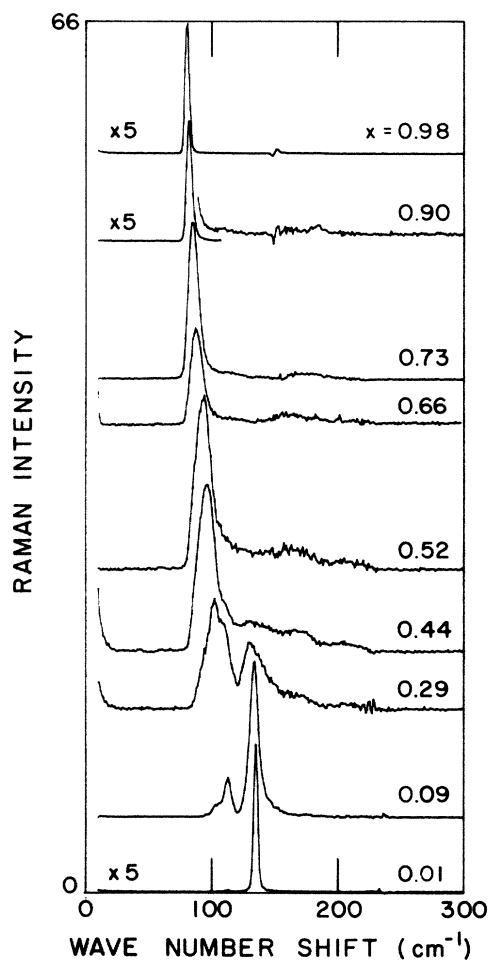


FIG. 4. Concentration dependence of the *E*-symmetry Raman spectrum of $\text{CdCl}_{2(1-x)}\text{Br}_{2x}$ recorded at 10 K with 457.9-nm laser excitation.

As mentioned earlier, the wave-vector dependence of the optic-mode frequencies in CdCl_2 -type crystals is small, so it is a reasonable approximation to consider a molecular model for the unit cell, i.e., the interaction between unit cells is assumed to be negligible. Consideration

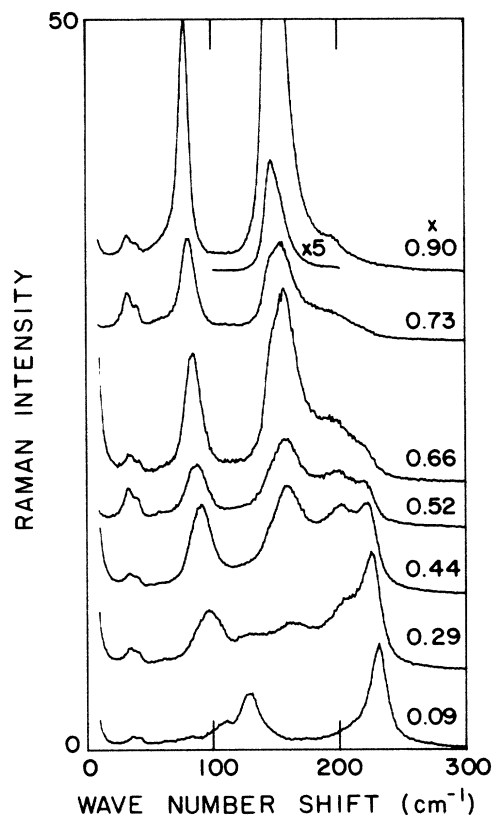


FIG. 5. Concentration dependence of the (*ZX* + *ZY*) Raman spectrum of $\text{CdCl}_{2(1-x)}\text{Br}_{2x}$ recorded at 300 K with 476.5-nm laser excitation.

of the layered structure of CdCl_2 leads to the conclusion that the molecular unit of importance is not the Cl-Cd-Cl formula unit, but rather one of the form $\text{Cl}_3\text{-Cd-Cl}_3$, where the halogen trios are the nearest neighbors to the metal ion. The corresponding entity in the mixed crystal is thus $\text{Cl}_m\text{Br}_{3-m}\text{-Cd-Cl}_n\text{Br}_{3-n}$ ($m, n = 0, 1, 2, 3$) and this gives rise to ten different molecular units as listed in Table I.

TABLE I. Different molecular units in $\text{CdCl}_{2(1-x)}\text{Br}_{2x}$, their probability of occurrence in the absence of clustering, and their Raman-active vibrational frequencies calculated in the averaged nearest-neighbor model and from experiment ($x = 0.44$).

Nearest-neighbor composition	Probability of occurrence	Component frequencies (cm^{-1})			
		<i>E</i>		<i>A</i>	
		Calc.	Expt.	Calc.	Expt.
$\text{Cl}_3\text{-Cd-Cl}_3$	$(1-x)^6$	135	130	234	224
$\text{Cl}_2\text{Br-Cd-Cl}_3$	$6x(1-x)^5$	119		210	215
$\text{Cl}_2\text{Br-Cd-Cl}_2\text{Br}$	$9x^2(1-x)^4$	109.5	109	194	204
$\text{Cl}_3\text{-Cd-ClBr}_2$	$6x^2(1-x)^4$	106.5		191.5	197
$\text{Cl}_2\text{Br-Cd-ClBr}_2$	$18x^3(1-x)^3$	100		180	183
$\text{Cl}_3\text{-Cd-Br}_3$	$2x^3(1-x)^3$	96.5		178	
$\text{ClBr}_2\text{-Cd-ClBr}_2$	$9x^4(1-x)^2$	93	96	168.5	172
$\text{Cl}_2\text{Br-Cd-Br}_3$	$6x^4(1-x)^2$	91.5		168	
$\text{ClBr}_2\text{-Cd-Br}_3$	$6x^5(1-x)$	86		158.5	160
$\text{Br}_3\text{-Cd-Br}_3$	x^6	80.5		150	148

TABLE II. Calculated force constants for the A_{1g} and E_g phonons in CdCl_2 and CdBr_2 using frequencies measured at 10 K.

Crystal	Phonon symmetry	Phonon frequency (cm^{-1})	Force constant ($10^{-11} \text{ N m}^{-1}$)
CdCl_2	E_{1g}	135.0	3.82
	A_{1g}	234.0	11.4
CdBr_2	E_{1g}	80.5	3.05
	A_{1g}	150.0	10.6

The frequencies of the A and E Raman-active modes in the mixed crystal may be estimated from those of the pure crystals as follows. The normal modes of the A_{1g} and E_g phonons in CdCl_2 -type crystals¹² indicate that their frequencies, ω , may be written simply as $\omega_X^2 = k_X/M_X$, where k_X is the force constant and M_X the mass of halogen X . Using the Raman frequencies measured at 10 K, we obtain the values for k listed in Table II. In order to calculate the frequencies for the different molecular units in the mixed crystal we take average halogen masses given by

$$M_1 = \frac{1}{3}[mM_{\text{Cl}} + (3-m)M_{\text{Br}}] \quad (1)$$

and

$$M_2 = \frac{1}{3}[nM_{\text{Cl}} + (3-n)M_{\text{Br}}] \quad (2)$$

for each end of the unit. Because the force constants vary slightly in going from CdCl_2 to CdBr_2 we also form their averages,

$$k_1^\gamma = \frac{1}{3}[mk_{\text{Cl}}^\gamma + (3-m)k_{\text{Br}}^\gamma] \quad (3)$$

and

$$k_2^\gamma = \frac{1}{3}[nk_{\text{Cl}}^\gamma + (3-n)k_{\text{Br}}^\gamma], \quad (4)$$

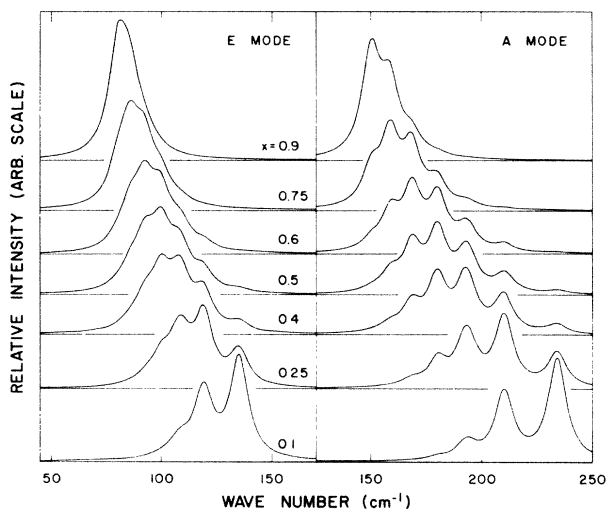


FIG. 6. Calculated concentration dependence of the Raman scattering by A - and E -symmetry modes in $\text{CdCl}_{2(1-x)}\text{Br}_{2x}$ assuming a random halogen distribution and a Lorentzian damping of 10 cm^{-1} .

where γ is the symmetry label. For the symmetric cases, where $m=n$, the molecular unit frequencies are given by $\omega_\gamma^2 = (k_1^\gamma + k_2^\gamma)/(M_1 + M_2)$, but for the remaining non-symmetric cases the Cd^{2+} ion is allowed to move. The frequencies are then obtained by considering the linear XYZ molecule problem with solutions²⁰

$$\omega_{\gamma_a}^2 + \omega_{\gamma_b}^2 = k_1^\gamma \left[\frac{1}{M_1} + \frac{1}{M_{\text{Cd}}} \right] + k_2^\gamma \left[\frac{1}{M_{\text{Cd}}} + \frac{1}{M_2} \right] \quad (5)$$

and

$$\omega_{\gamma_a}^2 \omega_{\gamma_b}^2 = k_1^\gamma k_2^\gamma (M_1 + M_2 + M_{\text{Cd}})/M_1 M_2 M_{\text{Cd}}, \quad (6)$$

where the lower-frequency solution to these simultaneous equations corresponds to the vibration of interest here. Using these equations, we obtain for each symmetry species the ten component frequencies listed in Table I.

For comparison with experiment we also calculated the relative intensities of the ten components by assuming the Raman intensity is proportional to the probability of occurrence of each cluster, as given in Table I. The resulting concentration dependence of the scattering, for a random halogen distribution in the mixed crystals, is depicted in Fig. 6, where for convenience the A and E modes are assumed to have the same Raman polarizability and each mode has arbitrarily been assigned a Lorentzian damping of 10 cm^{-1} . This diagram clearly shows the salient features of the ANN model: The components are fixed in frequency, while the apparent frequency shift in the overall peak intensity arises from the different concentration dependencies in the intensities of individual components.

The approach in our ANN model is related to the model developed by Verleur and Barker^{21,22} to describe the long-wavelength lattice vibrations in $\text{GaAs}_y\text{P}_{1-y}$ and $\text{CdSe}_y\text{S}_{1-y}$, and later extended by them to mixed crystals with the fluorite structure.^{7,8} The essential feature of the Verleur and Barker model was the enumeration of the various possible distinct nearest-neighbor complexes in each case. In computing the probability of occurrence of each of these complexes as a function of the concentration index y , a clustering parameter β was introduced to allow for a possible preferred clustering of like ions at a local (i.e., nearest-neighbor) level rather than a random distribution in the mixed crystal. The five distinct units for the tetrahedral nearest-neighbor complexes treated by Verleur and Barker correspond to the ten distinct molecular units we have identified in the $\text{CdCl}_{2(1-x)}\text{Br}_{2x}$ case. The possibility of a preferred clustering of like halogens in our layered mixed crystals is considered in the next section.

V. DISCUSSION

In general terms the ANN model is successful in explaining the mixed-crystal experimental results. The number of peaks and shoulders observed in the A spectrum at intermediate x values certainly exceeds three, and is as high as eight for some concentrations, as is shown in Figs. 2 and 3. Not as many distinct peaks are observed in the E spectra (see Fig. 4), presumably because the component frequencies lie close together. The band envelopes

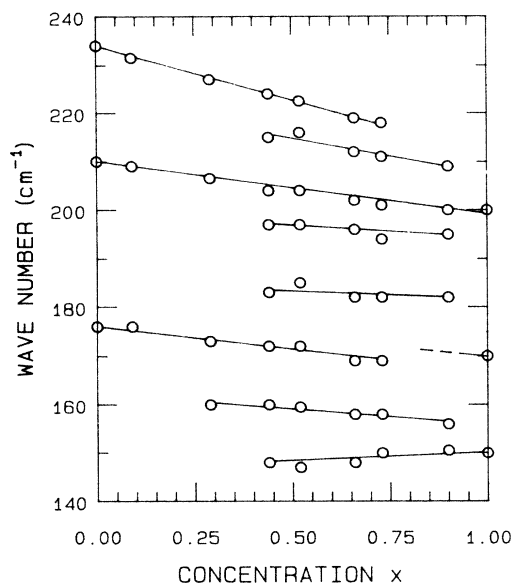


FIG. 7. Peak frequencies at 10 K of lines in the *A*-symmetry Raman spectrum of $\text{CdCl}_{2(1-x)}\text{Br}_{2x}$ versus x . The lines link corresponding features for different x values.

of the original spectra and of Figs. 3 and 4 indicate further lines are present beneath the dominant peaks. The concentration dependences of the component frequencies, including shoulder features, are presented in Figs. 7 and 8. Because of the proximity of several of the predicted mode frequencies and the natural linewidth of each component, one does not expect to resolve all components for any one concentration. Thus a prediction of ten components for each symmetry species is comparable with experiment.

The computed frequencies are in reasonable agreement with experimental observations (see Table I) considering the approximations made. The peak frequencies of several prominent components do appear to vary linearly with concentration (see Figs. 7 and 8) which indicates some intercell coupling is occurring, as would be expected. Interactions between the closely spaced modes of the same symmetry must also be expected, although such interactions were not allowed for. The differences between calculated and experimental frequencies are thus not surprising.

Although the predicted behavior for the concentration dependence of the Raman scattering intensity appears to be in qualitative agreement with the experimental results for *E* symmetry, a closer comparison of Figs. 4 and 6 reveals some discrepancies. The *A* symmetry scattering clearly does not follow the expected pattern. At intermediate concentrations there is a minimum in the intensity at frequencies for which the intensity should show a peak (compare Figs. 3 and 6 for $x \sim 0.5$). This result was not expected, considering other successful features of the ANN model and the success of the model (including intensities) in a parallel study of $\text{CdBr}_{2(1-x)}\text{I}_{2x}$.²³ We propose that the intensity behavior with concentration indicates a preferred clustering of bromide (or chloride) ions within the halogen layers. Such a proposition would be

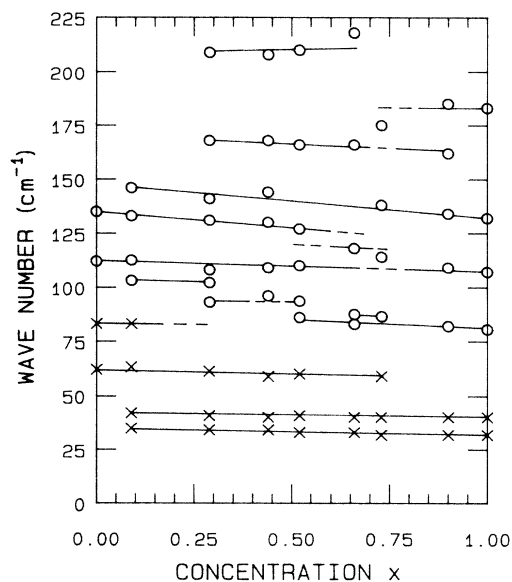


FIG. 8. Peak frequencies of lines in the *E*-symmetry Raman spectrum of $\text{CdCl}_{2(1-x)}\text{Br}_{2x}$ versus x : measurements at 300 K (crosses) or 10 K (open circles). The lines link corresponding features for different x values.

difficult to prove conclusively. We do know that the crystals are homogeneous over a larger scale, for several reasons. An examination of different parts of one crystal by Raman scattering and by chemical analysis proved the sample had a uniform concentration. Crystals grown with the same nominal concentration consistently gave an actual concentration close to the nominal value. Mixed crystals were readily grown for any concentration. These facts indicate that the bromide and/or chloride ions mix well and that any clustering must be on a small scale. The scale from our model would be of the order of one molecular unit. The origin for such clustering probably lies in the difference in the c'_0/a'_0 lattice-constant ratios for the pure compounds (see Sec. II) and the ease with which each halogen lattice can accommodate the cadmium layers.

In an attempt to quantify the proposed clustering, we have investigated the introduction of a clustering parameter β . Following Verleur and Barker,²¹ we define β such that the probability of finding a Cl^- ion next to another Cl^- ion (P_{ClCl}) and the probability of finding a Br^- ion next to another Br^- ion (P_{BrBr}) are

$$P_{\text{ClCl}} = (1-x) + \beta x, \quad (7)$$

$$P_{\text{BrBr}} = x + \beta(1-x). \quad (8)$$

These are equivalent to Eqs. (1) and (2) of Ref. 21, and the computation of the probabilities for the occurrence of each of the ten basic units in $\text{CdCl}_{2(1-x)}\text{Br}_{2x}$ proceeds along similar lines, although the extension from four to six nearest-neighbors is not trivial. The resulting cluster probabilities are listed in the Appendix. It is not clear that such a one-parameter treatment of clustering is adequate for the layered crystal structure considered here. The probability for clustering of like ions within a given

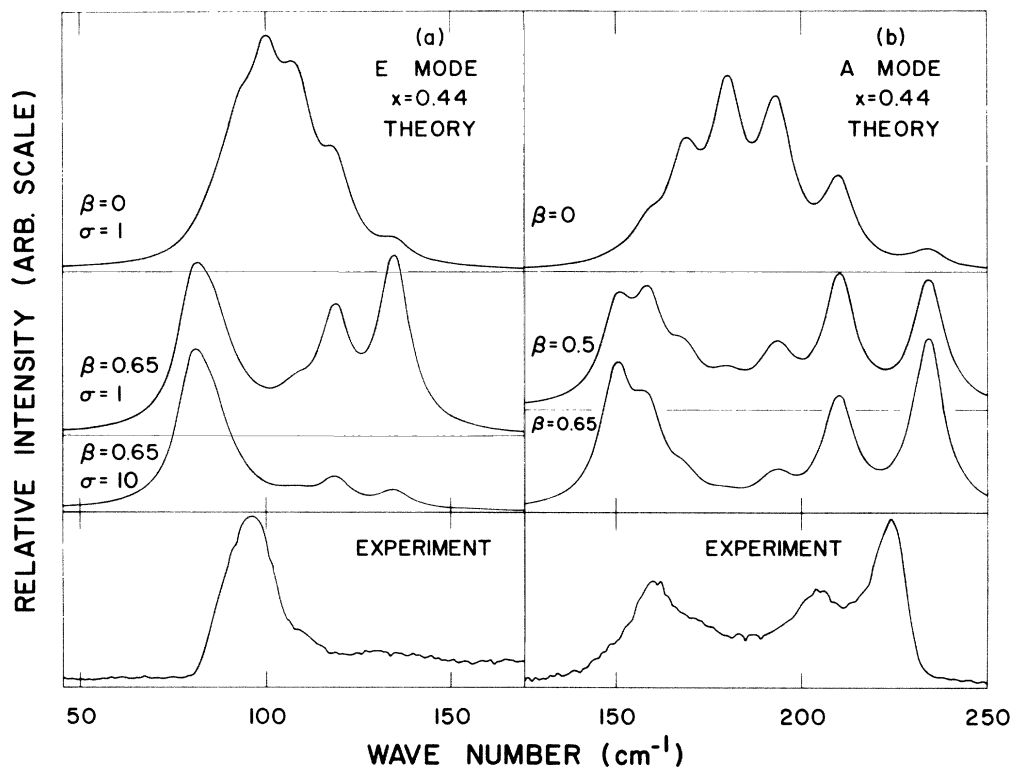


FIG. 9. Raman spectra of (a) *E* and (b) *A* modes in $\text{CdCl}_{1.12}\text{Br}_{0.88}$ compared with theory for different values of the clustering parameter β and the scattering strength ratio $\sigma = S_{\text{Br}}/S_{\text{Cl}}$.

halogen layer may well differ from the probability for interlayer clustering of like halogens in a given $\text{Cl}_m\text{Br}_{3-m}$ - $\text{Cd-Cl}_n\text{Br}_{3-n}$ unit, but the added complication of a second clustering parameter is not justified at this stage.

In Fig. 9(b) we compare the observed *A*-mode scattering for $x = 0.44$, and the mode pattern predicted for $\beta = 0$ (no clustering), $\beta = 0.5$, and $\beta = 0.65$, using an arbitrary Lorentzian damping of 10 cm^{-1} as typical of the observed linewidths. The effect of clustering is clearly evident and a value of $\beta \sim 0.6$ gives a reasonable fit to the observed scattering. A similar comparison for other values of x shows, however, that no one value of β gives a satisfactory fit to the *A*-mode scattering throughout the concentration range. Generally $0.5 < \beta < 0.7$ gives the best fit for $x \leq 0.6$, reducing to $\beta < 0.5$ for $x \geq 0.66$, but this one-parameter clustering model has several deficiencies. In particular, no choice of β can explain the relative strength of the 200-cm^{-1} feature, which we have identified with clusters containing four chloride ions and two bromide ions, in the $x = 0.90$ and $x = 0.98$ spectra (see Fig. 10).

The situation of the *E*-mode scattering is even more unsatisfactory. Here a marked asymmetry appears in the strength of scattering from bromine-rich molecular units compared to chlorine-rich units in the mixed crystals. In Fig. 4 it is clear that bromine-rich nearest-neighbor clusters dominate the *E*-mode scattering for $x \geq 0.44$, although such asymmetry was not expected from comparison of the $x = 0.98$ and $x = 0.01$ spectra. In an attempt to accommodate this asymmetry, the computed cluster intensities were scaled by a factor $nS_{\text{Cl}} + (6-n)S_{\text{Br}}$, where

S_{Cl} and S_{Br} represent intrinsic chloride and bromide contributions to the *E*-mode scattering strength and n gives the number of chloride ions in each nearest-neighbor complex. A comparison of measured and computed *E*-mode scattering for $x = 0.44$ [Fig. 9(a)] suggests a best fit with $\beta \sim 0.6$ and $S_{\text{Br}} \sim 10S_{\text{Cl}}$. Such a $S_{\text{Br}}/S_{\text{Cl}}$ ratio tends to suppress the β dependence of the model, but gives a reasonable fit (with $\beta \sim 0.5$) for $x \geq 0.29$. The fit for $x = 0.09$ is not satisfactory, however, and again a close inspection of the $x = 0.98$ scattering (see Fig. 10) reveals unexpected strength for the $\text{Cl}_2\text{Br-Cd-Cl}_2\text{Br}$ unit (at 109

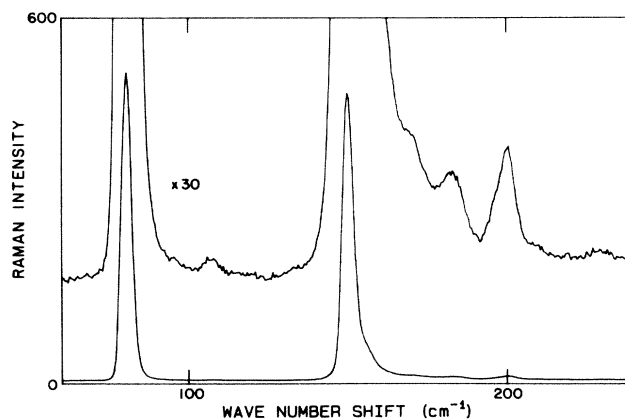


FIG. 10. Part of the $X(YY+YX)Z$ Raman spectrum of $\text{CdCl}_{0.04}\text{Br}_{1.96}$ recorded at 10 K.

cm^{-1}) as in the A -mode scattering.

In summary, the one-parameter clustering model considered here, although lending support to the clustering postulate, fails to provide a satisfactory explanation of the observed scattering throughout the entire concentration range $0 < x < 1$. The clustering in this layered structure is clearly of a more complex nature than that in the systems considered by Verleur and Barker.

Other weaker lines not considered above appear in the mixed crystals. They lie either between the Raman-active bands of E and A symmetry or below 85 cm^{-1} (see Figs. 5, 7, and 8). Low-frequency lines occur near 35, 42, and 61 cm^{-1} at 10 K, and are most evident in (YZ) or (XZ) polarization at 300 K (see Fig. 5), confirming that they have E symmetry. Their peak frequencies vary little with concentration, while their intensities are a maximum for $x \sim 0.5$. Their temperature dependencies, as shown for example in Fig. 1, suggest that the bands are first order in origin. As no optic modes are expected in this frequency region, we conclude that these lines are due to disorder-induced scattering from acoustic phonons, most probably at wave vectors near the Brillouin-zone boundary. Other CdCl_2 -type crystals possess zone-boundary acoustic modes at similar frequencies,¹⁰ but since the dispersion curves for CdCl_2 and CdBr_2 are unknown we cannot make definite assignments. One interesting feature is the weak concentration dependence in their frequencies. One possible explanation is that the 35- and 42-cm^{-1} features arise from cadmium bromide acoustic modes, while the 61-cm^{-1} feature and the 83-cm^{-1} line (seen only for $x = 0.01$ and $x = 0.09$ at 300 K) arise from the corresponding cadmium chloride modes. The apparent two-mode behavior is consistent with the proposed halogen clustering.

The higher-frequency lines are very broad. Those near 167 and 210 cm^{-1} again have E symmetry (see Fig. 4), have frequencies largely independent of concentration, and their intensities are a maximum for $x \simeq 0.5$. This again is consistent with disorder-induced one-phonon scattering. Infrared-active modes are expected in this frequency region [for example, the CdCl_2 (CdBr_2) E_u (TO) and A_{2u} (LO) modes occur at 156 (113) and 239 (184) cm^{-1} , respectively²⁴] but the fact that the mixed-crystal frequencies are insensitive to concentration is inconsistent with an assignment to zone-center infrared modes. A more detailed understanding of these lines must await knowledge of the phonon dispersion curves.

VI. CONCLUSION

A Raman spectral study of the mixed crystal $\text{CdCl}_{2(1-x)}\text{Br}_{2x}$ has revealed a complicated multimode behavior for the phonon concentration dependence which arises from the layered nature of the crystal structure. An averaged nearest-neighbor model, which incorporates the local metal-halogen structure, predicts a ten-mode behavior (for each pure-crystal optical mode) in the mixed crystal. Extension of the model to include the effects of different next-nearest-neighbors in each halogen layer would increase beyond ten the number of distinct contributing modes for each phonon type. Interactions between the molecular groupings would also need to be considered

in a more detailed interpretation. Nevertheless, our simple ANN model satisfactorily accounts for the general features of the observed concentration dependence of the scattering. The distribution of intensities for the components of the scattering suggests that preferred clustering of chloride or bromide ions occurs in the mixed crystal. It is conjectured that the clustering arises as a result of differences in the lattice constants of CdCl_2 and CdBr_2 . It would be informative to carry out an extended x-ray-absorption fine-structure study of $\text{CdCl}_{2(1-x)}\text{Br}_{2x}$ to investigate clustering, as recently performed on other mixed crystals.^{25,26}

In view of the interesting new results obtained from $\text{CdCl}_{2(1-x)}\text{Br}_{2x}$ and from $\text{CdBr}_{2(1-x)}\text{I}_{2x}$,²³ where clustering effects were not observed, it would be interesting to study mixed crystals of other layered structures such as the $\text{Cd}(\text{OH})_2$ one.⁹

ACKNOWLEDGMENTS

We wish to thank R. A. Ritchie for growing the crystals and V. Clancy (Chemistry Division, National Research Council) for the chemical analysis of the mixed crystals. This work was supported in part by the New Zealand University Grants Committee. One of us (R.W.G.S.) acknowledges the hospitality of the National Research Council of Canada while on study leave.

APPENDIX: CLUSTER PROBABILITIES

We summarize here the results for the probabilities of occurrence (f_n) of the various molecular units (as in Table I) upon inclusion of the clustering parameter β . For $\text{Cl}_3\text{-Cd-Cl}_3$,

$$f_1 = (1-x)^6 + \beta x(1-x)[3(1-x)^4 + 3(1-x)^2 + 2x - 1] + 3\beta^2 x^2(1-x)^2[(1-x)^2 + 1] + \beta^3 x^3(1-x)^3.$$

For $\text{Cl}_2\text{Br-Cd-Cl}_3$,

$$f_2 = 6(1-\beta)x(1-x)^2[(1-x)^3 + 2\beta x(1-x)^2 + \beta x + \beta^2 x^2(1-x)].$$

For $\text{Cl}_2\text{Br-Cd-Cl}_2\text{Br}$,

$$f_3 = 9(1-\beta)^2 x^2(1-x)^4 + 9\beta(1-\beta)^2 x^3(1-x)^3.$$

For $\text{Cl}_3\text{-Cd-ClBr}_2$,

$$f_4 = 6(1-\beta)^2 x^2(1-x)^4 + 6\beta(1-\beta)^2 x^3(1-x)^3.$$

For $\text{Cl}_2\text{Br-Cd-ClBr}_2$,

$$f_5 = 18(1-\beta)^3 x^3(1-x)^3.$$

For $\text{Cl}_3\text{-Cd-Br}_3$,

$$f_6 = 2(1-\beta)^3 x^3(1-x)^3.$$

For $\text{ClBr}_2\text{-Cd-ClBr}_2$,

$$f_7 = 9(1-\beta)^2 x^4(1-x)^2 + 9\beta(1-\beta)^2 x^3(1-x)^3.$$

For $\text{Cl}_2\text{Br-Cd-Br}_3$,

$$f_8 = 6(1-\beta)^2 x^4(1-x)^2 + 6\beta(1-\beta)^2 x^3(1-x)^3.$$

For $\text{ClBr}_2\text{-Cd-Br}_3$,

$$f_9 = 6(1-\beta)x^2(1-x)[x^3 + 2\beta x^2(1-x) + \beta(1-x) + \beta^2 x(1-x)^2].$$

For $\text{Br}_3\text{-Cd-Br}_3$,

$$f_{10} = x^6 + \beta x(1-x)(3x^4 + 3x^2 - 2x + 1) + 3\beta^2 x^2(1-x)^2(x^2 + 1) + \beta^3 x^3(1-x)^3.$$

*Permanent address: Department of Physics, University of Canterbury, Christchurch, New Zealand.

¹I. F. Chang and S. S. Mitra, *Adv. Phys.* **20**, 359 (1971).

²A. S. Barker, Jr. and A. J. Sievers, *Rev. Mod. Phys.* **47**, Suppl. 2, S1 (1975).

³C. Barta, G. F. Dobrzanski, G. M. Zinger, M. F. Limonov, and Yu. F. Markov, *Fiz. Tverd. Tela (Leningrad)* **24**, 2952 (1982) [*Sov. Phys.—Solid State* **24**, 1672 (1982)], and references therein.

⁴A. Zwick, G. Landa, M. A. Renucci, R. Carles, and A. Kjekshus, *Phys. Rev. B* **26**, 5694 (1982).

⁵N. M. Gasanly, A. F. Goncharov, N. N. Melnik, and A. S. Ragimov, *Phys. Status Solidi B* **120**, 137 (1983).

⁶G. M. Zinger, I. P. Ipatova, and A. V. Subashiev, *Fiz. Tekh. Poluprovodn.* **10**, 479 (1976) [*Sov. Phys.—Semicond.* **10**, 286 (1976)].

⁷A. S. Barker, Jr. and H. W. Verleur, *Solid State Commun.* **5**, 695 (1967).

⁸H. W. Verleur and A. S. Barker, Jr., *Phys. Rev.* **164**, 1169 (1967).

⁹R. W. G. Wyckoff, *Crystal Structures*, 2nd Ed., (Wiley-Interscience, New York, 1963), Vol. 1, p. 270.

¹⁰G. Benedek and A. Frey, *Phys. Rev. B* **21**, 2482 (1980).

¹¹S. Nakashima, H. Yoshida, T. Fukumoto, and A. Mitsuishi, *J. Phys. Soc. Jpn.* **31**, 1847 (1971).

¹²D. J. Lockwood, *J. Opt. Soc. Am.* **63**, 374 (1973).

¹³D. J. Lockwood and J. H. Christie, *Chem. Phys. Lett.* **9**, 559 (1971).

¹⁴G. Mischler, D. Bertrand, D. J. Lockwood, M. G. Cottam, and S. Legrand, *J. Phys. C* **14**, 945 (1981).

¹⁵D. J. Lockwood, G. Mischler, A. Zwick, I. W. Johnstone, G. C. Psaltakis, M. G. Cottam, S. Legrand, and J. Leotin, *J. Phys. C* **15**, 2973 (1982).

¹⁶N. L. Rowell, D. J. Lockwood, and P. Grant, *J. Raman Spectrosc.* **10**, 119 (1981).

¹⁷K. S. Chao, Physics Department, University of Canterbury, New Zealand, Report No. 79-4, 1979 (unpublished).

¹⁸C. W. Tomblin, G. D. Jones, and R. W. G. Syme, *J. Phys. C* **17**, 4345 (1984).

¹⁹I. W. Johnstone, D. J. Lockwood, and G. D. Jones, *Solid State Commun.* **39**, 395 (1981).

²⁰G. Herzberg, *Infrared and Raman Spectra of Polyatomic Molecules* (Van Nostrand, New York, 1945), p. 173.

²¹H. W. Verleur and A. S. Barker, Jr., *Phys. Rev.* **149**, 715 (1966).

²²H. W. Verleur and A. S. Barker, Jr., *Phys. Rev.* **155**, 750 (1967).

²³R. E. M. Vickers, R. W. G. Syme, and D. J. Lockwood, *J. Phys. C* **18**, 2419 (1985).

²⁴J. A. Campbell and R. E. M. Vickers, *J. Phys. C* **16**, 999 (1983).

²⁵J. C. Mikkelsen, Jr. and J. B. Boyce, *Phys. Rev. B* **28**, 7130 (1983).

²⁶J. B. Boyce and J. C. Mikkelsen, Jr., *Phys. Rev. B* **31**, 6903 (1985).